Accounting for Horizontal Reinforcement in FE Modeling of RC Shear Walls Using Cyclic Softened Membrane Model (Case Study of a Full Scale Shaking Table Test)

H. Soltani
Islamic Azad University, Najafabad Branch, Isfahan, Iran

M.A. Rahgozar
University of Isfahan, Isfahan, Iran

ABSTRACT:
This paper presents simulation of nonlinear dynamic response of a full-scale seven-story reinforced concrete shear wall in a shaking table test under base excitations representing four earthquake records of increasing intensity, conducted by NEES-UCSD (2006). This current study compares two different FE simulation models for the shear wall test specimen, namely: fiber-section-model and the cyclic softened membrane model (CSMM). CSMM is more sophisticated in accounting for the horizontal reinforcement, and in modeling of the softening effect on the concrete in compression due to the tensile strain in the perpendicular direction, the softening effect on the concrete in compression under reversed cyclic loading, the opening and closing of cracks, which are taken into account in the unloading and reloading stages. It is concluded that in the fiber section model although the computer runs are faster and more stable, the CSMM model provides more accurate and representative nonlinear structural responses.

Keywords: RC shear wall, fiber section model, cyclic softened membrane model (CSMM), shaking table, horizontal reinforcement .

1. INTRODUCTION

Reinforced concrete (RC) shear walls are the main source of providing stiffness and strength in concrete structures during earthquakes. Therefore a realistic evaluation of their inelastic static as well as dynamic responses is essential. So many experimental and analytical studies have been performed in order to develop analytical models which predict the inelastic response of RC walls. Many studies have focused on refining those analytical models which produce more accurate results. These models must be for example capable of accounting for the movement of neutral axis, shear deformations and interaction between shear and axial forces with bending moments in concrete sections. Some researchers such as Martinelli and Filippou (2009) have attempted to simulate analytically a full scale seven-story reinforced concrete shear wall in a shaking table test under base excitations representing four earthquake records of increasing intensity, conducted by NEES-UCSD (2006). They used 2D fiber section model (Figure 3.2) and reported a relative accuracy for their model predictions except some deviation in certain parts of their analytical results compared to the experimental values, for example in base shears and overturning moments. This current study, using the same finite element modeling as other researchers, identifies the sources of some of these deviations and proposes improvements to this simulation study. The main causes of these deviations are considered to be: 1) a lack of more accurate model for the true behavior of RC shear walls under cyclic loading; and 2) not accounting for the effects of the horizontal steel confining/shear reinforcements. Fortunately, the cyclic softened membrane model (CSMM) which addresses both of the aforementioned issues was recently added to OpenSees software. The cyclic softened membrane model (CSMM), proposed by Hsu and Mo (2010) is usually used for plane stress four node elements of RC shear walls. In addition to that, it is capable of rationally predicting the pinching effect in the hysteretic loops, the shear stiffness, the shear ductility and the energy dissipation capacities of the panel elements. The characteristics of the concrete constitutive laws attached to CSMM model include: (1) the softening effect on the concrete in compression due to the tensile strain in the perpendicular direction; (2) the softening effect on the concrete in compression under reversed cyclic loading; (3) the opening and closing of cracks, which are taken into account in the unloading and reloading stages. The main objective in this study is to compare the nonlinear dynamic responses of the test structure models using fiber section model as used by Martinelli and Filippou (2009), and CSMM as proposed here in this study.

2. DESCRIPTION OF TEST STRUCTURE

The test structure is a portion of a 7-story residential building incorporating structural walls as the lateral force-resisting system. The structure was built at full-scale as shown in Figure 2.1. The design base shear for the building calculated from the displacement-based design methodologies was 14% of the weight of the structure. This is approximately one-half the base shear force obtained from the 1997 Uniform Building Code [UBC 1997] (Panagiotou and Restrepo, 2007). The test structure comprised of a main 3.65 m long rectangular wall and two transverse structural elements: a 4.88m wide flange wall and a precast segmental pier column. The width of the web wall was 203 mm at the first and seventh levels and 152mm elsewhere. The width of the flange wall is 203mm at the first level and 152mm elsewhere. Figure 2.1 depicts a view of the test specimen. The foundation and the floor plan view of the specimen are shown in Figure 2.2. The 3.65m×8.13m simply supported slab of each level rests on the walls and on auxiliary gravity columns. At each level, the flange wall is connected to the slab and to the web wall through a slotted connection. The segmental pier column is connected to the slab through a pin–pin horizontal steel truss. For the gravity columns, high-strength steel pin–pin rods grouted in 102mm pipes were used. Regarding the slab connection to the web wall and the flange wall, a slotted connection on both sides was established in order to minimize the moment transfer and the coupling between the web wall and the flange wall. In contrast the slotted connection was designed in order to guarantee a diaphragm action in the longitudinal and transverse directions (Panagiotou and Restrepo, 2007). Figure 2.3 shows the slab connection details. Tunnel steel forms were used for the construction of the walls and slabs. The concrete had a compressive cylinder strength of 28Mpa and an average elastic modulus of 29 GPa, while the steel was A615 grade 60 (Martinelli and Filippou, 2009). The reinforcement details of the web and the flange walls are shown in Figure 2.4.

Figure 2.1. View of Test Specimen.

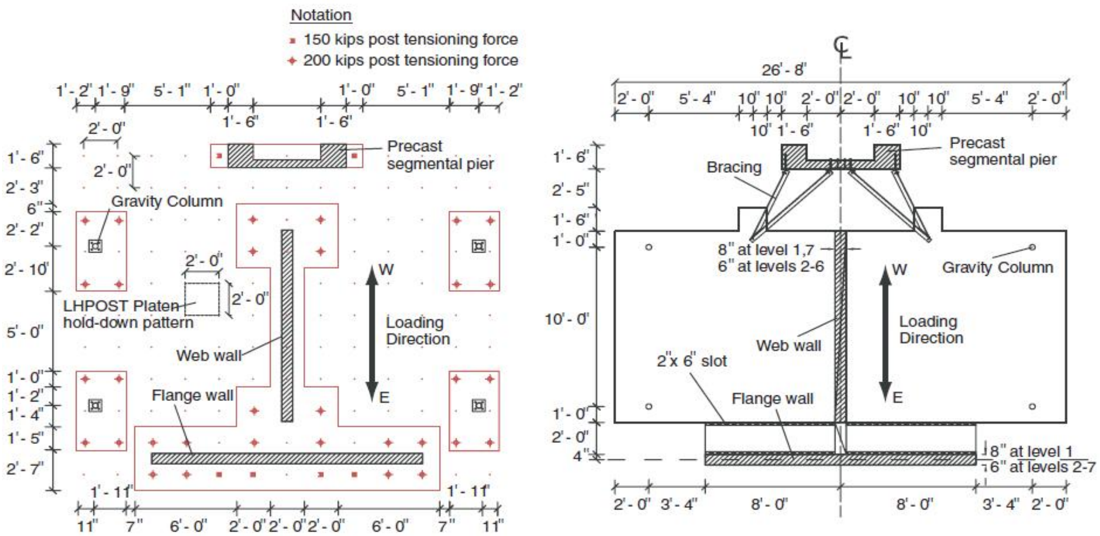

Figure 2.2. View of foundation and typical floor plan (U.S. customary units)

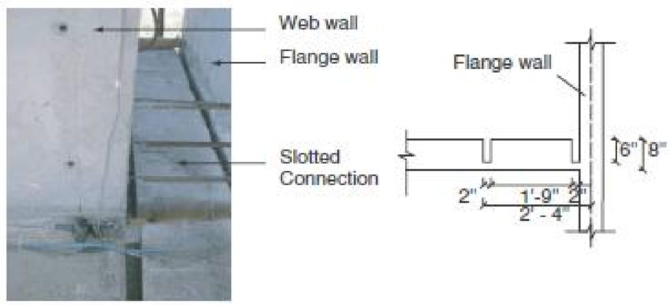

Figure 2.3. View of the slotted connection (U.S. customary units).

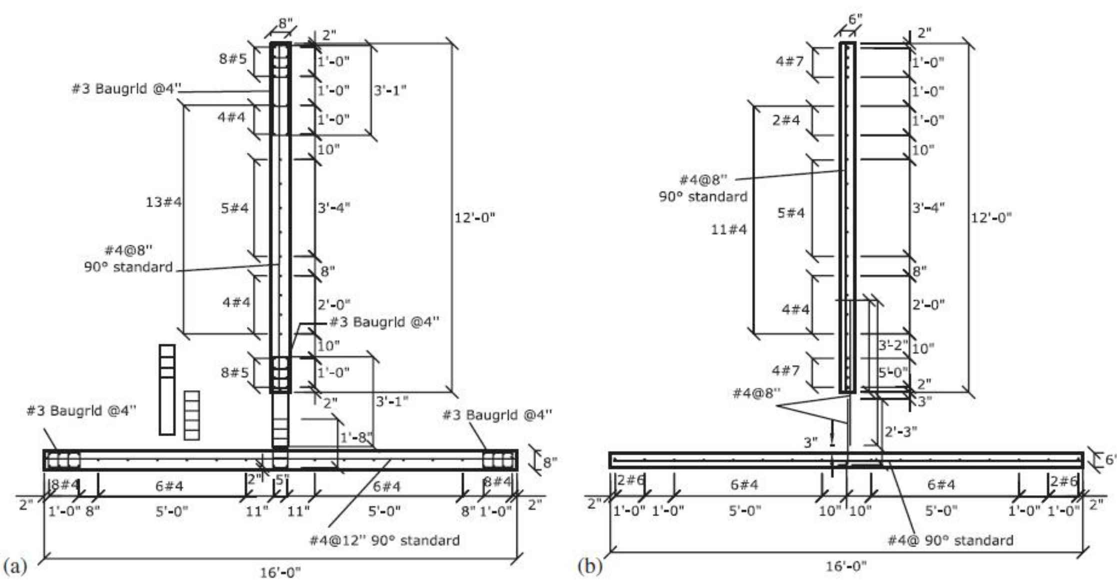

Figure 2.4. View of the Reinforcement details for the wall specimen: (a) first level and (b) levels 2–6 (U.S .customary units).

3. FIBER SECTION MODEL

Fiber section model (Figure 3.2) is based on a nonlinear beam-column element with distributed inelasticity with several integration points along the span. In which, the shear wall is represented by 2D beam–column elements with fiber discretization of the cross-section that accounts for the interaction of axial force and bending moment.

Similar to Martinelli and Filippou (2009), the Rayleigh constants are therefore so set that the damping ratio for the first two flexural modes become 1%. The material type Concrete02 from OpenSees library is used to model both the unconfined (cover) and confined concrete regions. For the concrete fibers (or layers in a 2D model), the modified Kent–Park model was used for the response in compression (Kent and Park 1971, Park and Priestley 1982). It consists of an ascending parabolic branch and a descending linear part for strains greater than the strain corresponding at peak stress. To simulate the behavior in tension and the tension stiffening effect, a linear elastic branch is followed by a linear softening branch up to zero stress in tension. The steel fibers follow the nonlinear model of Menegotto and Pinto (1973) which is the material type Steel02 from OpenSees library.

Figure 3.1 illustrates material behaviors for steel and concrete, both in tension and compression. The steel yielding strength is 450MPa and the concrete properties are given in Table 3.1.

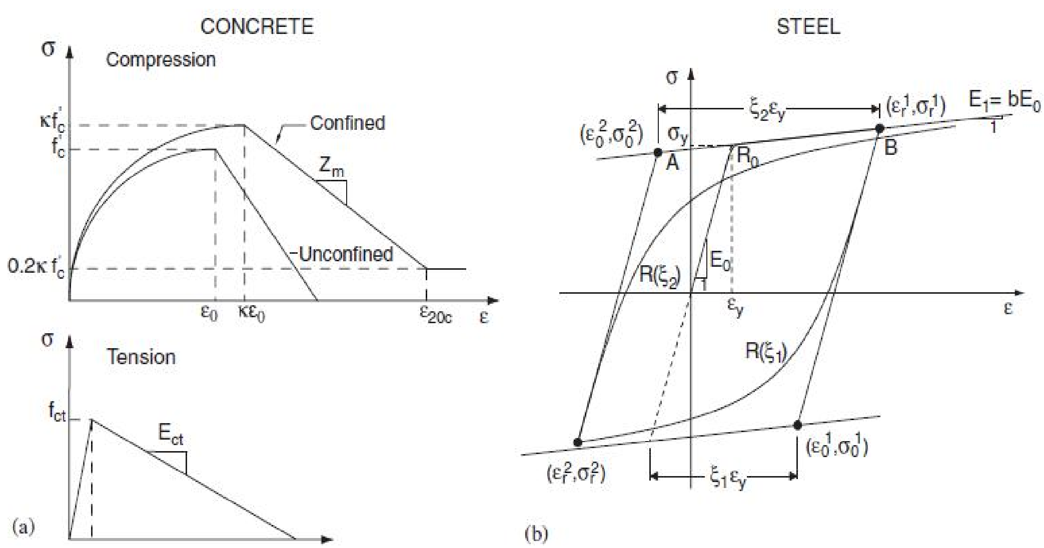

Figure 3.1. Constitutive material models: a) concrete02 b) steel02 (OpenSEES 2008).

Table 3.1. Concrete material properties assumed in the analyses (Martinelli and Filippou 2009).

Concrete Type	f'_c (MPa)	ε_0 $\times 10^{-3}$	ε_u $\times 10^{-3}$	κ	Z_m	f_{ct} (MPa)	E_{ct} (MPa)
Unconfined	−37.9	−2.70	−5.09	1	376	3.8	2800
Confined	−45.8	−3.26	−30.3	1.21	30	3.8	2800

Both the web and flange walls are modeled as force-based nonlinear beam-column elements with fiber cross-sections. In fiber model, there are a number of control cross-sections along the element. Each cross-section is subdivided into concrete and steel fibers where uniaxial stress-strain laws are used to describe the response of the material in the longitudinal direction (parallel to the element axis). These sections are located at the control points of the numerical integration scheme (Figure 3.2).

The footings under the web and flange walls were very large and remain elastic during the test. Thus, a single linear elastic element was used under each wall. The properties of these linear elements were based on the gross section with a Young modulus of concrete of E_c=27500MPa close to the average measured value (Martinelli and Filippou, 2009). The precast column and the braces were designed to remain elastic during the tests. In the model, the precast column element was represented with a linear elastic frame element and the braces with linear elastic truss elements (Martinelli and Filippou, 2009). The slotted connection, similar to Martinelli and Filippou, 2009, is modeled by a truss element which is capable of transferring axial load only and not moment. This could be a source of error since in reality during the test, these slotted connections show some flexural resistance while in the FE analyses their effects are ignored. The force based nonlinear beam-column element is used for modeling the web and flange walls. The FE model of the test structure for fiber model is illustrated in Fig. 4.3a.

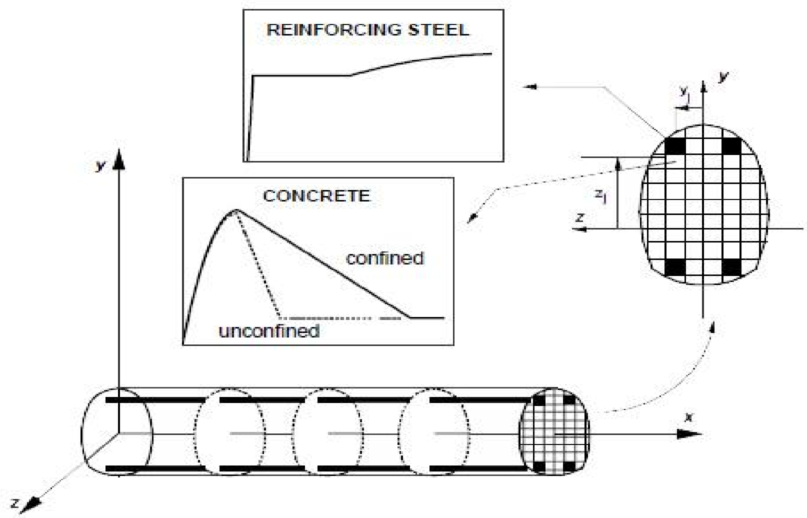

Figure 3.2. Fibre beam-column element (Spacone and Filippou 1991).

4. CYCLIC SOFTEND MEMBRANE MODEL (CSMM)

The cyclic softened membrane model (CSMM) was proposed by Mansour and Hsu (2005). Of the main features of this model is to account more accurately for behavior of RC shear walls under cyclic loading. It also accounts for the effects of the horizontal steel confining/shear reinforcements.

This model is capable of rationally predicting the pinching effect in the hysteretic loops, the shear stiffness, the shear ductility and the energy dissipation capacities of the panel elements. Three material models namely SteelZ01, ConcreteZ01 and RCPlaneStress in OpenSees are developed for CSMM. SteelZ01 and CencreteZ01 are uniaxial material modules, in which the uniaxial constitutive relationships of steel and concrete specified in the CSMM are defined. The RCPlaneStess is implemented with quadrilateral element to represent the four node reinforced concrete membrane elements. The uniaxial materials steelZ01 and concreteZ01, are essential components in the RCPlane modules.

The cyclic uniaxial constitutive relationships of concrete Z01 in compression and tension are given in Figure 4.1. The characteristics of these concrete constitutive laws include: (1) the softening effect on the concrete in compression due to the tensile strain in the perpendicular direction; (2) the softening effect on the concrete in compression under reversed cyclic loading; (3) the opening and closing of cracks, which are taken into account in the unloading and reloading stages. Cyclic uniaxial constitutive relationships of embedded mild steel bars are given in Figure 4.1. The steel module SteelZ01 needed in the CSMM incorporates both the envelope and the unloading/reloading pattern of uniaxial constitutive relationships of embedded mild steel (Mansour and Hsu 2001, Mansour and Hsu 2005).

For the structural model using CSMM, the web wall is comprised of two end columns and the main part of the wall. The end columns are modeled by fiber section model and therefore the material properties shown in Figure 3.1 are applicable. The flange wall is also modeled using fiber section model with same properties in Figure 3.1. The material properties corresponding to the four node finite elements of the main part of the web wall are SteelZ01 and ConcreteZ01 shown in Figure 4.1.

Of the main superiorities of CSMM model is the consideration of the horizontal reinforcements and their impact on nonlinear-cyclic behavior of RC walls. A sensitivity study on FE mesh of the wall panels is run with 2, 6 and 12 elements, in order to find an optimized number of finite elements in each panel, which led to adoption of the 12 element mesh shown in Fig.4.3b.

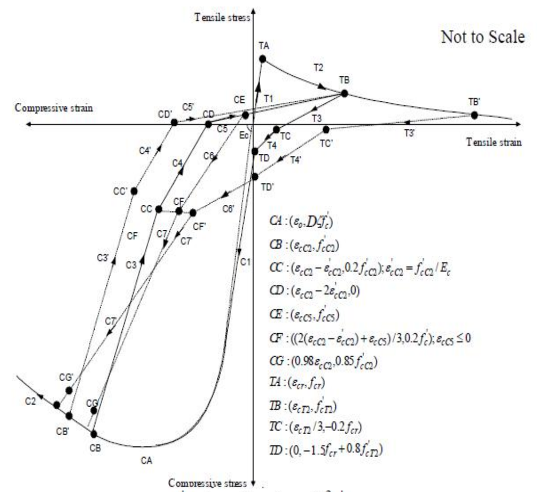

(Stage C1) $\sigma^c = D\zeta f_c^{'}\left[2\left(\frac{\bar{\varepsilon}}{\zeta\varepsilon_o}\right)-\left(\frac{\bar{\varepsilon}}{\zeta\varepsilon_o}\right)^2\right] \quad 0\le|\bar{\varepsilon}|\le|\zeta\varepsilon_o|$

(Stage C2) $\sigma^c = D\zeta f_c^{'}\left[1-\left(\frac{\bar{\varepsilon}/\varepsilon_o-1}{4/\zeta-1}\right)^2\right] \quad |\bar{\varepsilon}|>|\zeta\varepsilon_o|$

where

$\zeta=\frac{5.8}{\sqrt{f_c^{'}(MPa)}}\frac{1}{\sqrt{1+400\bar{\varepsilon}_T^{'}/\eta^{'}}}\le 0.9; D=1-0.4\frac{\varepsilon_c^{'}}{\varepsilon_o}\le 1.0; \eta^{'}=\frac{\rho_t f_{ty}-\sigma_t}{\rho_\ell f_{\ell y}-\sigma_\ell}\le 1.0$

(Stage T1) $\sigma^c = E_c\bar{\varepsilon}$ if $0\le\bar{\varepsilon}<\varepsilon_{cr}$

(Stage T2) $\sigma^c = f_{cr}\left(\frac{\varepsilon_{cr}}{\bar{\varepsilon}}\right)^{0.4}$ if $\bar{\varepsilon}>\varepsilon_{cr}$

(Unloading and Reloading Stages) $\sigma^c=\sigma_i^c+E_{cc}(\bar{\varepsilon}_i-\bar{\varepsilon}); E_{cc}=\frac{\sigma_i^c-\sigma_{i+1}^c}{\bar{\varepsilon}_i-\bar{\varepsilon}_{i+1}}$

a)

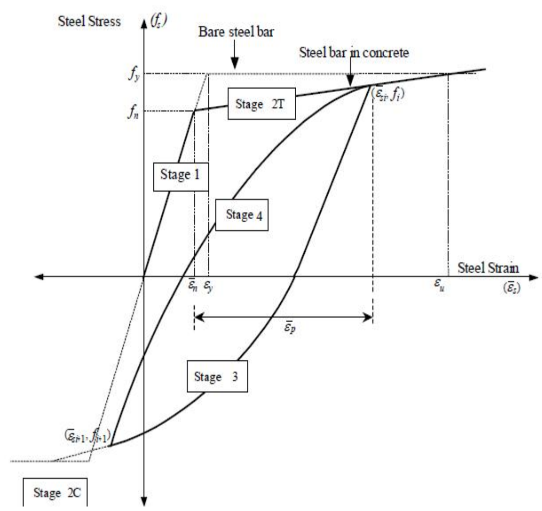

(Stage 1) $f_s = E_s\bar{\varepsilon}_s \quad (\bar{\varepsilon}_s\le\bar{\varepsilon}_n)$

(Stage 2T) $f_s = f_y\left[(0.91-2B)+\left(0.02+0.25B\frac{\bar{\varepsilon}_s}{\varepsilon_y}\right)\right] \quad (\bar{\varepsilon}_s>\bar{\varepsilon}_n)$

where $B=\frac{1}{\rho}\left(\frac{f_{cr}}{f_y}\right)^{1.5}$ and $\rho\ge 0.5\%$; $\bar{\varepsilon}_n=\varepsilon_y(0.93-2B)$

(Stage 2C) $f_s=-f_y \quad (f_s\le -f_y)$

(Stage 3 and Stage 4) $\bar{\varepsilon}_s-\bar{\varepsilon}_{si}=\frac{f_s-f_i}{E_s}\left[1+A^{-R}\left|\frac{f_s-f_i}{f_y}\right|^{R-1}\right]$

where $A=1.9k_p^{-0.1}$, $R=10k_p^{-0.2}$ and $k_p=\frac{\bar{\varepsilon}_p}{\bar{\varepsilon}_n}$

b)

Figure 4.1. Material properties linked to CSMM, a) ConcreteZ01 b) SteelZ01(Mo and Zhong 2006).

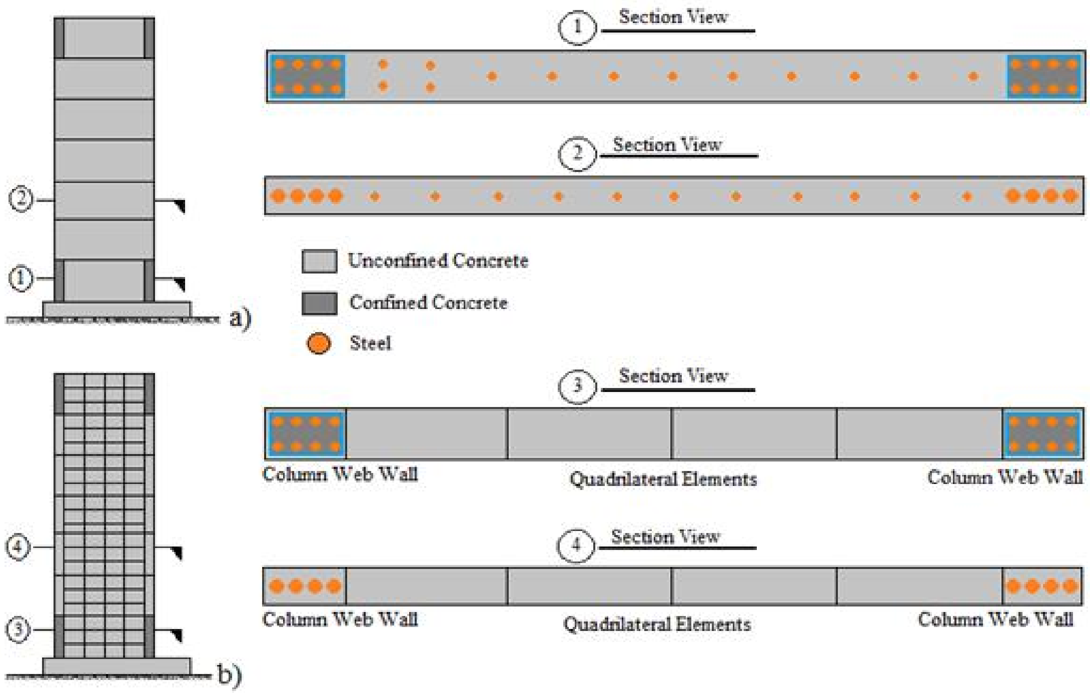

Figure 4.2. Side view and cross section of web wall, a) Fiber model, b) CSMM

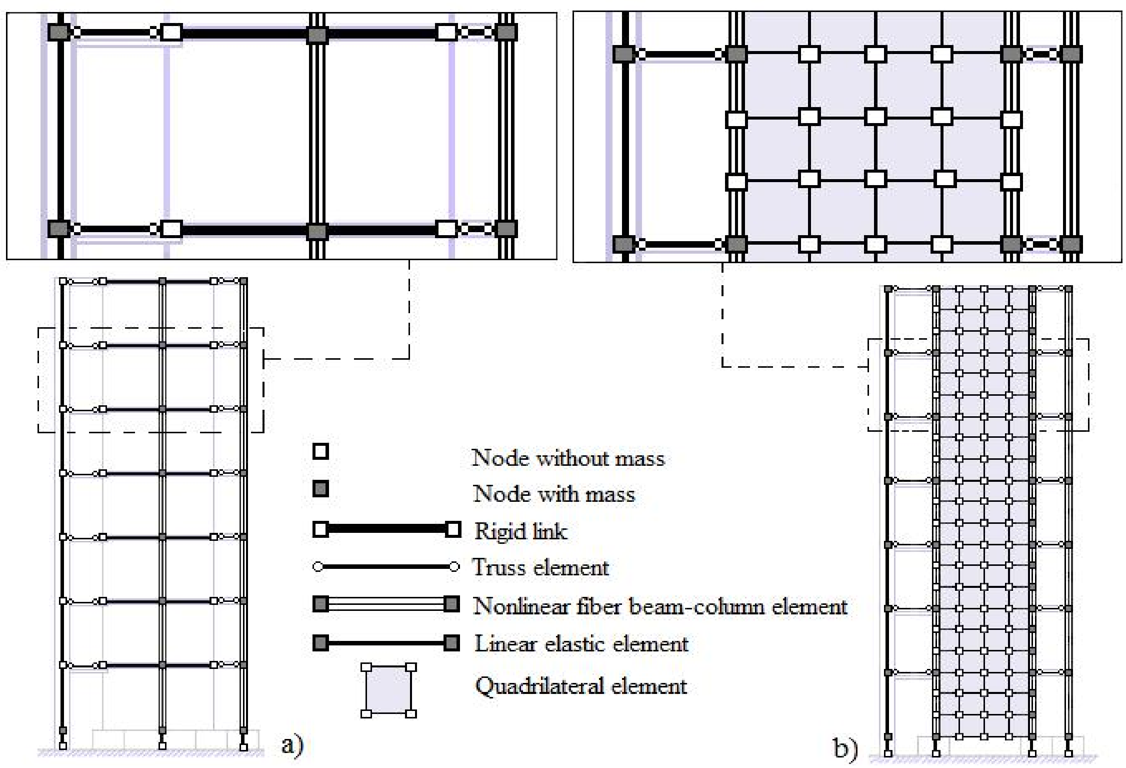

Figure 4.3. Analytical models of the shear wall specimen.(a) Fiber model, (b) CSMM with 12 elements in each wall panel.

5. INPUT GROUND MOTIONS AND DYNAMIC ANALYSES

The program included low amplitude 0.5-25 Hz band-clipped white noise tests, a low intensity earthquake, EQ1, two medium intensity earthquakes, EQ2 and EQ3, and a large intensity earthquake, EQ4. The low intensity earthquake record was the Van Nuys longitudinal component from the 1971 San Fernando earthquake, with PGA = 0.15g. The two medium intensity records were the Van Nuys transverse component record from 1971 San Fernando earthquake, with PGA = 0.27g, and the Oxnard Boulevard Woodland Hill longitudinal component from the Northridge 1994 earthquake, with PGA = 0.34g. The large intensity record is the Sylmar Olive View Medical Centre 360o component record from the 1994 Northridge earthquake, with PGA = 0.91g (Figure 5.1).

The gravity loads were applied first in a static analysis, followed by the dynamic analysis of the models. Similar to the previous studies, the dynamic analyses of the specimen were conducted with a single continuous sequence of concatenated acceleration records from EQ1 to EQ4. All nonlinear time-history analyses adopted the Newmark time integration method of constant acceleration (γ =0.5, β =0.25), with a time step equal to Δt = 1/120 s. Similar to the original simulation study by Martinelli and Filippou (2009), Rayleigh damping constants were so set that damping ratio for the first two flexural modes becomes 1%.

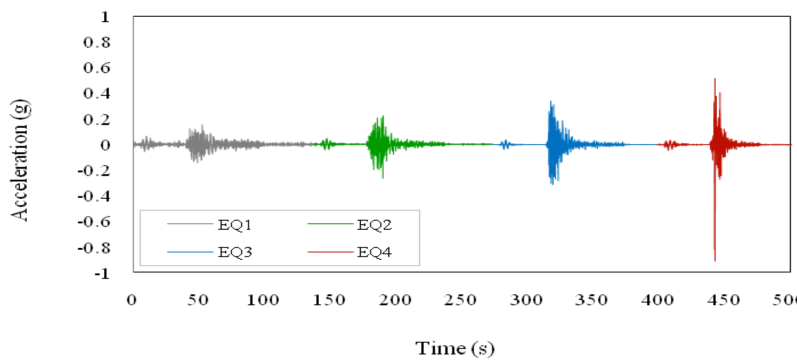

Figure 5.1. Ground motions EQ1–EQ4.

6. RESULTS AND DISCUSSIONS

Figures 6.1(a-d) depict the envelope of the maximum values for floor lateral displacement, inter-story drift, story shear force, and overturning moment for the two analytical models defined in this work as well as the experimental values, different markers are used for each input motion. The experimental shear force and the overturning moment were evaluated at the centre line of the web wall and took into account the inertial effects of all elements of the structure. Table 6.1 provides a comparison of the maximum experimental responses with those obtained by time-history analyses using both fiber as well as CSMM models.

The reported story shear values in Figure 6.1(c) are based on the static restoring forces of all elements and does not account for the damping force contribution. These are compared with the experimental values, which are determined from the product of the story mass and the measured horizontal floor acceleration, and thus include the damping force contribution (Martinelli and Filippou, 2009). This may cause considerable deviation of the analytical results from the experimental ones.

The effects of the gravity columns in this study, although very important to the overall structural response, but similar to the original simulation study by Martinelli and Filippou (2009), are ignored. This is because in 2D analysis, without simplifying assumptions, it is impossible to account for them. However, the influence of the gravity columns and floor slab on the overall force-displacement response of the test building was evident during testing, and was confirmed by Panagioutou and

Restrepo (2006) using a pushover analysis of the building. By ignoring their effects, the lateral force resisting system capability could be underestimated up to 24% compared to the lateral force resistance of the test building.

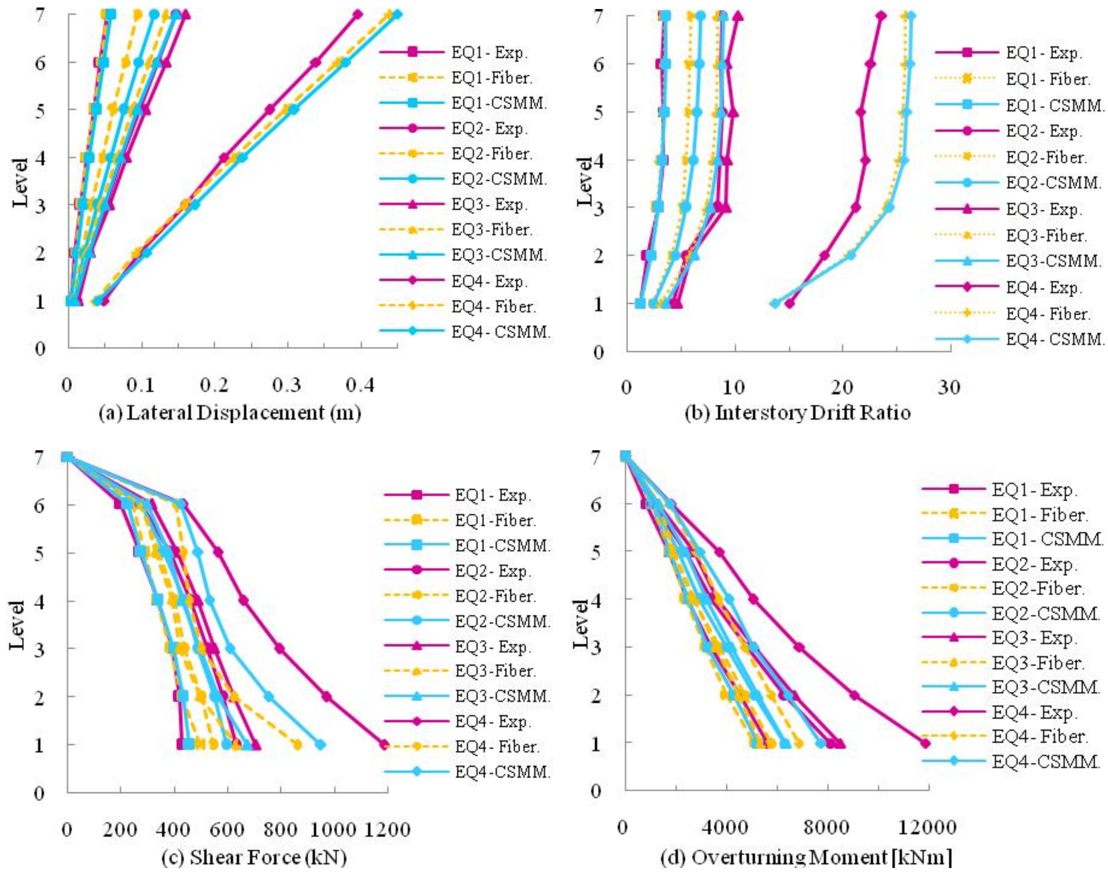

Figure 6.1. Envelops of experimental and the two analytical models results:(a) lateral displacement, (b) inter-story drift, (c) shear force, (d) overturning moment.

Table 6.1. Maximum response values from time-history analysis and test measurements.

	EQ1			EQ2			EQ3			EQ4		
	Exp	Com	Err	Exp	Com	Err	Exp	Com	Err	Exp	Com	Err
U_{top} (mm)	52			146			160			395		
Fiber Model		53	1.92		93.26	-36.12		133.5	-16.56		437.5	9.71
CSMM Model		56.8	9.23		117.3	-19.66		147.1	-8.06		449.3	13.75
$Drift_{top}(\times 10^{-3})$	3.46			8.84			10.03			23.60		
Fiber Model		3.46	0.00		5.85	-33.82		8.39	-18.54		25.8	9.32
CSMM Model		3.54	2.31		6.75	-23.64		8.92	-11.07		26.17	10.89
V_{base} (KN)	425			628			704			1185		
Fiber Model		494	16.24		545	-13.22		628	-10.8		858	-27.59
CSMM Model		456	7.29		594	-5.41		672	-4.55		947	-20.08
M_{base} (KNm)	5606			8093			8490			11839		
Fiber Model		5106	-8.92		5785	-28.52		5340	-37.1		6850	-42.14
CSMM Model		5265	-6.08		6299	-22.17		6348	-25.23		7743	-34.6

7. SUMMARY AND CONCLUSIONS

In this study a seven story full scale RC concrete shear wall test specimen was modeled using two different FE models, subjected to four earthquakes of increasing maximum acceleration from 0.15 to 0.93g, representative of low, medium, and high levels of excitation. In the first model, similar to previous studies, fiber section model was used, while in the second model, the CSMM is adopted. This comparison covered the envelopes of floor displacement, interstory drift, story shear, and overturning moment over the height of the structure (Fig. 6.1) and the maximum values of base shears, Vbase, base overturning moments, Mbase, top floor displacement, top floor interstory drift, for each earthquake motion (Table 6.1).

The results for Vbase and Mbase in the second model are considerably closer to the experimental values. This proximity is more owed to the use of CSMM model. In general all the displacement and force responses are closer to the experimental values when the RC shear wall is modeled by CSMM than modeled by fiber model. Also for higher intensity earthquakes the error in Vbase and Mbase values is higher, which can attributed to the lateral load resistant capacity of the gravity columns in the experimental test while neglected in the analytical models. Also, in general, the story displacements and story drift ratios are higher when modeled by CSMM compared to fiber model. The latter is due to a better account of concrete cracking and their opening and closing of cracks in CSMM model. In brief it is concluded that because of providing more accurate nonlinear structural responses and its consideration of horizontal reinforcements, CSMM is more reliable for nonlinear dynamic response analyses of RC shear wall structures.

REFERENCES

Kent DC, Park R. (1971). Flexural member with confined concrete. Journal of Structural Division, Proceedings of the American Society of Civil Engineers. 97(ST7):1969–1990.

Menegotto, M., and E. Pinto. (1973). Method of analysis for cyclically loaded reinforced concrete plane frames including changes in geometry and non-elastic behavior of elements under combined normal force and bending, Proceedings, IABSE Symposium. Lisbon, Portugal..

Park R, Priestley MJN, Gill WD. (1982). Ductility of square-confined concrete columns. ASCE Journal of the Structural Engineering. **108(4):**929–950.

Taucer, Fabio F, E Spacone, FC Filippou. (1991). A Fiber Beam-Column Element for Seismic Response Analysis of Reinforced Concrete Structures. Report No. UCB/EERC-91/17, Earthquake Engineering Research Centre, College of Engineering, University of California, Berkeley.

Mansour, M., Lee, J. Y., and Hsu, T. T. C. (2001). Constitutive laws of concrete and steel bars in membrane elements under cyclic loading. Journal of Structural Engineering, ASCE, **127**, 12, 2001, 1402-1411.

Englekirk, R. E. (2003). Seismic Design of Reinforced and Precast Concrete Buildings. John Wiley & Sons, Inc., Hoboken, New Jersey.

Mansour, M. and Hsu, T. T. C. (2005). Behavior of reinforced concrete elements under cyclic shear: part 1 - theoretical Model. Journal of Structural Engineering, ASCE, 44-53.

Mansour, M. and Hsu, T. T. C. (2005). Behavior of reinforced concrete elements under cyclic shear: part 2 – experiments. Journal of Structural Engineering, ASCE, 54-65.

Mo,Y.L., Zhong, J. and Laskar, A. (2006). Performance-based Design of RC Shear Walls Using Cyclic Softened membrane Model. 2nd FIB Congress, Session 8 Seismic Design of New Concrete Structures, Naples, Italy.

Restrepo, J. I. and Preti, M. (2006). A Two-level Displacement-based Design Methodology for Structural Wall Buildings. 2nd fib Congress, Naples, Italy.

Panagiotou, M., J. I. Restrepo and J. P. Conte. (2007). Shake table test of a 7 story full scale reinforced concrete structural wall building slice - Phase I: Rectangular wall. Report No SSRP-07/07, University of California, San Diego.

McKenna F, Fenves GL, Scott MH. (2008) .Open System for Earthquake Engineering Simulation, University of California, Berkeley. Available from: http://opensees.berkeley.edu.

Martinelli, P. and Filippou, F. (2009). Simulation of the shaking table test of a seven-story shear wall building. Earthquake Engineering and Structural Dynamics. **38**, 587-607.

Hsu, Thomas T. C. and Mo, Y. L. (2010).Unified Theory of Concrete Structures. 2nd Edition, John Wiley & Sons, Ltd, United Kingdom, 518 pp.